



Illuminating Potential of Diphenyltin(IV) Dithiocarbamate Compounds for Pharmacological Applications: Synthesis, Structural Elucidation, *In-silico* and Cytotoxicity Study on A549 Human Lung Cancer Cells

NURUL AMALINA ABD AZIZ¹, NORMAH AWANG^{1*}, NURUL FARAHANA KAMALUDIN¹, NUR NAJMI MOHAMAD ANUAR¹, ASMAH HAMID¹ and KOK MENG CHAN²

¹Center for Toxicology and Health Risk Studies, Faculty of Health Sciences, Universiti Kebangsaan Malaysia, Jalan Raja Muda Abdul Aziz, 50300 Kuala Lumpur, Malaysia.

²Product Stewardship and Toxicology, Petroliaam Nasional Berhad, Level 13, Tower 1, PETRONAS Twin Towers, KLCC, 50088 Kuala Lumpur, Malaysia.

*Corresponding author E-mail: norm@ukm.edu.my

<http://dx.doi.org/10.13005/ojc/400309>

(Received: February 26, 2024; Accepted: May 17, 2024)

ABSTRACT

The process of development and optimization of anticancer drugs entails the design, synthesis, and elucidating of a diverse range of compounds. Among these are organotin(IV) dithiocarbamate metal complexes, which offer promising potential as anti-cancer agents. Recent studies have underscored the potential of these complexes to exert encouraging anti-proliferative activities against cancer cells, which can be attributed to their distinctive molecular structures and interactions with malignant tissues. This study aimed to refine the chemical constitution of Ph_2Sn (*N*-ethyl-*N*-benzylidithiocarbamate) through the application of cutting-edge analytical methods, including elemental and spectral analysis (infrared (IR) and NMR spectroscopy). Following optimization, the bioactivity of the newly designed compounds was evaluated on A549 human lung cancer cells utilizing standardized MTT assays to bring a better understanding of the structure-activity relationship (SAR). Our results indicate that these compounds display augmented cytotoxicity vis-à-vis current platinum-based chemotherapeutics, cisplatin, thereby highlighting their potential as an innovative alternative to conventional anti-cancer therapies.

Keywords: Organotin(IV) dithiocarbamate complexes, Spectral analysis, Cytotoxicity, Structure-activity relationship (SAR), A549 human lung cancer cells.

INTRODUCTION

In 1965, Dr. Barnett Rosenberg's discovery of cisplatin marked a breakthrough in cancer

treatment, catalyzing a new era in drug development. This chance finding not only expanded the therapeutic landscape but also represented a pivotal moment in oncological research. The unique chemistry of metal



complexes, characterized by redox reactivity, metal-ligand interactions, configurational arrangements, and Lewis acidity, positions them ideally to address diverse facets of cancer biology (Kumar Singh *et al.*, 2023). For over four decades, cisplatin has been a mainstay in treating non-small cell lung cancer (NSCLC), serving as a foundational therapy in this field (Bunn, 1989).

However, the evolution of cancer cells and their resistance to platinum-based treatments necessitate exploration of new strategies to combat this formidable challenge. Several factors constrain the full potential of these compounds, including issues with selectivity, pharmacokinetics, and solubility, diminishing their effectiveness as therapeutic agents (Islam *et al.*, 2021). Additionally, these compounds are associated with various toxicities, such as nephrotoxicity, hepatotoxicity, gastrotoxicity, myelosuppression, neurotoxicity, cardiotoxicity, and ototoxicity (Oun *et al.*, 2018).

Organotin compounds, particularly organotin(IV) compounds with direct tin-carbon bonds, offer promise among non-platinum metal-based compounds due to their low cytotoxicity and lack of cellular resistance, making them appealing for therapeutic use (Banti *et al.*, 2019). Research into their structure-activity-relationship (SAR) highlights key factors influencing their biological potency, including the availability of coordination sites on tin atoms, ligand-tin bond strength, and degradation rates through hydrolysis, as well as their capacity to coordinate with other molecules, the type and amount of organic groups (e.g., alkyl or aryl groups) attached to the tin atom, and the nature of the ligands involved (Iqbal *et al.*, 2017; Muhammad *et al.*, 2022).

Of particular interest are organotin(IV) dithiocarbamates, renowned for their bioactive properties (Haezam *et al.*, 2021) and unique stereochemical features that facilitate targeted delivery and extended residence time (Adeyemi and Onwudiwe, 2020). Synthesized tri- or diorganotin(IV) dithiocarbamates have shown heightened cytotoxicity compared to mono-organotin(IV) compounds (Abd Aziz *et al.*, 2023), attributed to increased tin(IV) ion coordination sites (Hadjikakou and Hadjiliadis, 2009). These compounds possess robust anticancer attributes by instigating programmed cell death, or apoptosis, through diverse cellular mechanisms.

They activate the intrinsic mitochondrial pathway following DNA damage, a crucial initiator of cell demise. Moreover, they impede vital cellular processes crucial for apoptosis, including cell cycle progression, resulting in arrests at different phases, such as G0/G1, S, and S-G2/M (Rasli *et al.*, 2023; Syed Anuar *et al.*, 2022). These findings highlight the potential therapeutic utility of organotin(IV) compounds in cancer treatment.

In light of their known anti-proliferative effects, this study examines the synthesis and potential therapeutic applications, particularly in the realm of cancer treatment, of $\text{Ph}_2\text{Sn}(N\text{-ethyl-}N\text{-benzylidithiocarbamate})$ (Fig. 1). Employing a range of analytical methods such as FT-IR, multiple NMR spectroscopy and elemental analysis, the structural characteristics of these newly synthesized compounds have been thoroughly investigated.

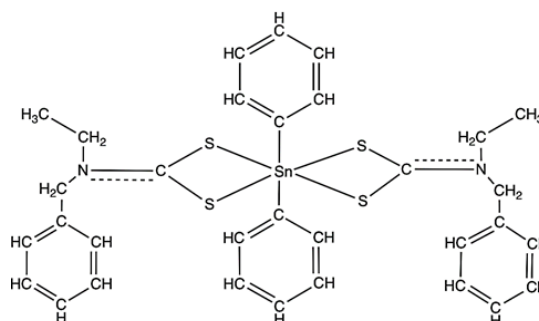


Fig. 1. The arrangement of atoms in $\text{Ph}_2\text{Sn}(N\text{-ethyl-}N\text{-benzylidithiocarbamate})$

MATERIALS AND METHODS

Comprehensive Analysis of ADMET Properties

The ADMET profile of $\text{Ph}_2\text{Sn}(N\text{-ethyl-}N\text{-benzylidithiocarbamate})$ was predicted using ADMETlab. We generated the SMILES strings for the individual moieties of this compound-diphenyltin(IV) and *N*-ethyl-*N*-benzylidithiocarbamate. These SMILES strings were added to the database and subsequently analyzed for their ADMET properties.

General

The secondary amine (*N*-ethylbenzylamine) and organotin(IV) chlorides were procured from Sigma Aldrich, carbon disulfide and ammonium solution (25%) were obtained from Merck, and acetone and ethanol (95%) were sourced from System Chemicals. These chemicals and solvents were used without further purification, adhering to the manufacturers' instructions. Melting points were

determined using the MPA120 EZ-Melt Automated Melting Point Apparatus. Subsequently, elemental analysis was conducted using a Perkin Elmer 2400 elemental analyzer to determine the percentages of C, H, N, and S present in the resulting compound. Infrared spectra were obtained using a Bruker Vertex 70v FT-IR Spectrometer within the frequency range of 4000 to 80 cm^{-1} . Additionally, ^1H , ^{13}C , and ^{119}Sn NMR spectra were recorded using 400 MHz Bruker Avance III NMR spectrometers with CDCl_3 as the solvent and tetramethylsilane as the internal standard at ambient temperature.

Synthesis of ligand (*N*-ethyl-*N*-benzylthiocarbamate)

We employed an "on-site" technique called "*in situ*" to synthesize the ligand dithiocarbamate. Initially, 30 millimoles of secondary amines were dissolved in 50 milliliters of ethanol and gently agitated for 30 minutes. Subsequently, the mixture comprising the secondary amine was combined with only two milliliters of ammonia solution and then stirred for another 30 minutes. By creating a basic atmosphere during this process, we facilitated the reaction's progression while simultaneously protecting the amine molecule (Oduлару and Ajibade, 2019). The subsequent procedure entailed adding 30 millimoles of carbon disulfide solution to 50 milliliters of ethanol as the solvent, followed by dissolution. Gradually, the solution was mixed and heated over 60 min at a temperature maintained below 4 degrees Celsius. This systematic approach led to the successful synthesis of the desired dithiocarbamate ligand.

Synthesis of $\text{Ph}_2\text{Sn}(\text{N-ethyl-N-benzylthiocarbamate})$

For the synthesis of $\text{Ph}_2\text{Sn}(\text{N-ethyl-N-benzylthiocarbamate})$, the ligand was combined with its corresponding metal salt in a precise ratio of 2:1. An exact amount of diphenyltin(IV) salt was gradually added to a solution containing dithiocarbamates, and the mixture was stirred carefully for two hours until a white solid formed. The resulting precipitate was filtered, washed thoroughly with chilled ethanol three times, and then dried in a desiccator.

Cell culture

The present study utilized A549 human lung cancer cells obtained from the American Type Culture

Collection (ATCC, Manassas, VA, USA). These cells were cultured in F12K medium supplemented with 10% fetal bovine serum (FBS) and 1% penicillin/streptomycin. Cell growth was carried out under standardized conditions within an atmosphere of 5% carbon dioxide and 37°C temperature to ensure optimal cell viability and proliferation.

Cell Viability Assay

We elucidate the anticancer potential of $\text{Ph}_2\text{Sn}(\text{N-ethyl-N-benzylthiocarbamate})$ against A549 human lung cancer cells using the MTT (3-(4,5-dimethylthiazo-2-yl)-2,5-diphenyltetrazolium bromide) assay, as described by Mosmann (1983). The MTT assay was performed by seeding 1×10^4 cells/well in 100 μL F-12K medium and incubated for an overnight period in CO_2 incubator. The next day, cells were subjected to varying concentrations of the test substance (compound), ranging from 0.16 μM to 5 μM , with the cisplatin treatment serving as a positive control and untreated cells acting as a negative control. Following this exposure, the plates were allowed to incubate for an additional 24 hours.

Subsequently, 20 μL of MTT was added to each well, followed by a 4-h incubation period at 37°C. Afterward, 180 μL of supernatant was removed, and any insoluble formazan crystals were solubilized by adding 180 μL of dimethyl sulfoxide (DMSO). The absorbance of the resulting solution was then measured at a wavelength of 570 nanometers using a Thermo Fisher Scientific Multiskan GO microplate reader.

To determine the percentage of cellular viability, we applied the following formula: Cell viability (%) = $100 \times (\text{Absorbance Compound} / \text{Absorbance Control})$. This information was then plotted as a function of compound concentration to illustrate the relationship between viable cell percentage and compound efficacy. Specifically, the IC_{50} signifies the amount required to induce a 50% decline in cell proliferation following a 24-h exposure period. These assays were conducted in triplicate, and the means \pm standard error of the mean (SEM) are reported as IC_{50} values (in micromolar units), which provide a quantitative measure of the compound's anticancer potential based on its ability to impair cell viability. Lower IC_{50} values correspond to more pronounced cytotoxicity towards cancer cells.

RESULTS AND DISCUSSION

Preparation of $\text{Ph}_2\text{Sn}(N\text{-ethyl-}N\text{-benzylidithio-carbamate})$

The compound was synthesized via an in situ method involving a two-stage chemical reaction. Specifically, we first synthesized ligand dithiocarbamates, followed by mixing them with diphenyltin(IV) in a 1:2 molecular ratio. The resulting $\text{Ph}_2\text{Sn}(N\text{-ethyl-}N\text{-benzylidithiocarbamate})$ was then purified via recrystallization to yield a single crystal sample. Subsequent elemental analysis revealed the composition of the synthesized compound as shown in Table 1. Notably, our compound demonstrated remarkable resistance to both atmospheric exposure and thermal degradation, displaying a melting point within the range of 108-110.9°C.

Table 1: Data on the elemental composition and physical characteristics of $\text{Ph}_2\text{Sn}(N\text{-ethyl-}N\text{-benzylidithiocarbamate})$

Chemical formula	Color	Yield	Found (Calculated)%			
			%C	%H	%N	%S
$(\text{C}_6\text{H}_5)_2\text{Sn}[\text{S}_2\text{CN}(\text{CH}_2\text{CH}_2(\text{C}_6\text{H}_5)(\text{CH}_2)_2)]_2$	White	32%	55.36 (55.41)	4.83 (4.94)	3.47 (4.04)	18.64 (18.49)

FT-IR and NMR characterization

According to Table 2 of our study, the Fourier Transform Infrared (FT-IR) spectroscopic characteristics of $\text{Ph}_2\text{Sn}(N\text{-ethyl-}N\text{-benzylidithiocarbamate})$ exhibit prominent peaks at 1480 and 996 cm^{-1} , which correspond to the $\nu(\text{C}\cdots\text{N})$ and $\nu(\text{C}\cdots\text{S})$ stretching modes (Martini *et al.*, 2021), respectively. Notably, these bands are found to be shifted towards higher frequencies likely as a result of the enhanced participation of the nitrogen lone pair in resonance following coordination of the

$N\text{-ethyl-}N\text{-benzylthiocarbamate}$ ligand with the tin ion (Onwudiwe *et al.*, 2015). Additionally, a solitary peak observed in $\nu(\text{C}\cdots\text{S})$ frequencies, it suggest that the ligand binds to the metal center in a symmetric bidentate chelating mode (Khan *et al.*, 2008). Furthermore, vibrations at 571 and 368 cm^{-1} can be ascribed to the (Sn-C) and (Sn-S) vibrational modes (Haezam *et al.*, 2021). These findings validate the successful synthesis of the organotin(IV) dithiocarbamates compound.

The NMR spectra of $\text{Ph}_2\text{Sn}(N\text{-ethyl-}N\text{-benzylidithiocarbamate})$ was carried out in a CDCl_3 solution. The ^1H , ^{13}C and ^{119}Sn NMR chemical shifts of compound are given in Table 3 and 4. The ^1H NMR data exhibited a signal at 5.060 ppm, which can be attributed to the shielding effect of the adjacent electronegative nitrogen atom on the methylene protons (Prakasam *et al.*, 2007). Additionally, multiple signals were detected between 7.945 and 7.969 ppm for the phenyl group of the dithiocarbamate (Ajibade *et al.*, 2011), while the phenyl group of the organotin moiety displayed signals between 7.270 and 7.528 ppm (Adeyemi *et al.*, 2022). Furthermore, triplets at 1.2384 ppm ($J = 7.1437$ Hz) were detected in the NMR spectrum which correspond to the methyl protons of the ethyl group (Onwudiwe *et al.*, 2016).

Table 2: FTIR analysis and physical data for the $\text{Ph}_2\text{Sn}(N\text{-ethyl-}N\text{-benzylidithiocarbamate})$

Compound	FTIR Analysis					
$(\text{C}_6\text{H}_5)_2\text{Sn}[\text{S}_2\text{CN}(\text{CH}_2\text{CH}_2(\text{C}_6\text{H}_5)(\text{CH}_2)_2)]_2$	$\nu(\text{C}\cdots\text{N})$	$\nu(\text{C}\cdots\text{S})$	$\nu(\text{Sn-C})$	$\nu(\text{Sn-S})$	$\nu(\text{N-C})$	$\nu(\text{C-H})$
	1480	996	571	368	1236	3064

Table 3: ^1H NMR spectrum for the $\text{Ph}_2\text{Sn}(N\text{-ethyl-}N\text{-benzylidithiocarbamate})$

Compound	Chemical shifts, δ (ppm)			
	N-R''(R'' = CH_3)	-NR'(R' = CH_2)	-NR'R aromatic	Sn-R(R = C_6H_5)
$(\text{C}_6\text{H}_5)_2\text{Sn}[\text{S}_2\text{CN}(\text{CH}_2\text{CH}_2(\text{C}_6\text{H}_5)(\text{CH}_2)_2)]_2$	1.2384, $J = 7.1437$ Hz	5.060	7.946 – 7.969	7.270 – 7.528

The chemical shift for N^{13}CS_2 at 200.49 ppm was the most significant signal in the ^{13}C NMR spectrum (Muthalib and Baba, 2014). This finding supports the notion that the presence of this system contributes significantly to the stabilization of complexes, ultimately resulting in reduced electron density. Additionally, the signals for ^{13}C NMR for diphenyltin group (127-130 ppm) were also detected in the same range as reported by Adeyemi *et al.*, (2020). Meanwhile,

the ^{13}C NMR signals of phenyl group present in dithiocarbamates exhibit multiplets within the chemical shift range of 134.29-151.51 ppm. Furthermore, the methylene carbon signal of the chelating dithiocarbamate was observed at 58.17 ppm (Mohamad *et al.*, 2016). The Sn signals revealed a hexacoordinate geometry around the tin center, as evidenced by the -495.85 ppm signal obtained through ^{119}Sn NMR spectroscopy (Adeyemi *et al.*, 2022).

Table 4: ^{13}C and ^{119}Sn NMR spectrum for the $\text{Ph}_2\text{Sn}(\text{N-ethyl-N-benzylidithiocarbamate})$

Compound	^{13}C , $\delta(\text{ppm})$				^{119}Sn , $\delta(\text{ppm})$
	N- CS_2	Sn-R(R= C_6H_5)	N- $\text{CH}_2\text{C}_6\text{H}_5$	N- CH_2CH_3	
$(\text{C}_6\text{H}_5)_2\text{Sn}[\text{S}_2\text{CN}(\text{CH}_2\text{CH}_3(\text{C}_6\text{H}_5)(\text{CH}_2))_2]$	200.49	127.64–130.2258.17	11.80	134.29,135.09,135.77,151.51	-495.85

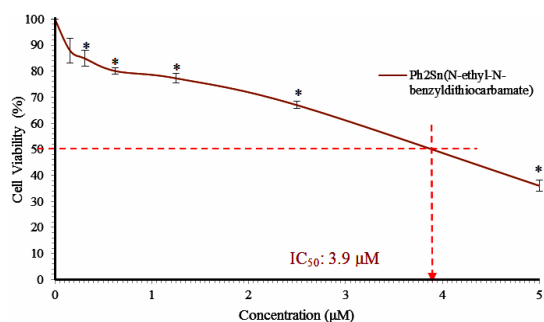
Cytotoxic evaluation of compound

Cellular metabolic activity was measured spectrophotometrically by monitoring the transformation of MTT into formazan, with increased absorbance indicating enhanced metabolism. Table 5 represents the relative IC_{50} values of $\text{Ph}_2\text{Sn}(\text{N-ethyl-N-benzylidithiocarbamate})$ and the positive control.

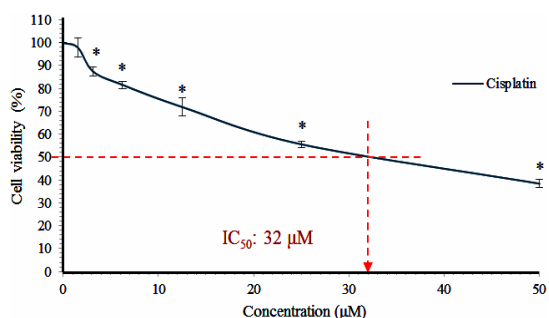
Table 5: IC_{50} values of the $\text{Ph}_2\text{Sn}(\text{N-ethyl-N-benzylidithiocarbamate})$ and cisplatin on A549 human lung cancer cells

IC_{50} (μM) \pm S.E.M	Cisplatin	$\text{Ph}_2\text{Sn}(\text{N-ethyl-N-benzylidithiocarbamate})$
	32 \pm 1.53	3.9 \pm 0.03

Our findings indicate that this compound possesses significant anticancer activity, as evidenced by its lower IC_{50} value compared to cisplatin, as depicted in Fig. 2 and 3. Consistent with this observation, we observed a dose-dependent hampering of cell growth when exposed to increase concentrations of the novel compound. Notably, the compound displayed a pronounced decline in cell viability beginning at 3 μM , suggesting its potential as an anticancer agent. Furthermore, previous research has also demonstrated the efficacy of novel diphenyltin(IV) dithiocarbamate complexes against various cell lines, including PC-3, HeLa, HT-29, and Jurkat E6.1 cells whereby these complexes exhibited substantial cytotoxic effects (Adeyemi *et al.*, 2022; Adeyemi and Onwudiwe, 2020; Haezam *et al.*, 2021; Kamaludin *et al.*, 2013).

**Fig. 2.** Effect of $\text{Ph}_2\text{Sn}(\text{N-ethyl-N-benzylidithiocarbamate})$ on the percentage of viability of A549 human lung cancer cells for 24 hours

*Statistically significant variance ($p < 0.05$) when compared to the negative control

**Fig. 3.** Effect of positive control, cisplatin on the percentage of viability of A549 human lung cancer cells for 24 hours

*Statistically significant variance ($p < 0.05$) when compared to the negative control

The potency of this compound as a cytotoxic agent is likely due to the presence of an aromatic (phenyl) group in organotin complexes, which enables π - π interactions with biological molecules such as proteins and nucleic acids (Kadu *et al.*, 2015). The π - π stacking interaction is a specific type of noncovalent interaction involving aromatic moieties containing π bonds. This interaction is a prerequisite in the development of drug delivery systems, particularly those bearing aromatic rings (Zhuang *et al.*, 2019). Furthermore, Liu *et al.*, (2017) demonstrated that these compounds are capable of intercalating into double-helix DNA structures in vitro. Given these results, it is essential to conduct thorough in vivo studies to assess both the safety and therapeutic potential of these compounds.

ADMET predicted profile

Using advanced computational tools like ADMETlab, we successfully predictive modelled the pharmacokinetics of $\text{Ph}_2\text{Sn}(\text{N-ethyl-N-benzylidithiocarbamate})$ (Table 6). Through examination of the distributions of various physicochemical properties of commercially available drugs, such as molecular weight, hydrophobicity, and polarity, it became evident that Ph_2Sn displays a substantial likelihood of being classified as a drug

candidate, with implications for oral absorption. These findings were further corroborated by applying The Rule of Five, a well-established filtering mechanism for assessing the oral bioavailability of

drugs, which entails restricting molecular weight to ≤ 500 g/mol, limiting logP to ≤ 5 , capping HBDs at ≤ 5 , and imposing a maximum of ≤ 10 HBAs (Guan *et al.*, 2019).

Table 6: ADMET predicted profile of Ph₂Sn(*N*-ethyl-*N*-benzylidithiocarbamate)

Model	Result of Diphenyltin(IV) (Value)	Probability	Result of N-ethyl-N-benzylidithiocarbamate (Value)	Probability Physicochemical property
Molecular weight	273.98	Orally well absorbed	211.05	Orally well absorbed
Amount of hydrogen bond donors (HBD)	0	Orally well absorbed	0	Orally well absorbed
Amount of hydrogen bond acceptors (HBAs)	0	Orally well absorbed	1	Orally well absorbed
Absorption				
Lipid Bilayer solubility (logP)	3.936	Permeable, Less solubility	2.327	Permeable, High solubility
Human Intestinal Absorption (HIA)	0.017	HIA+	0.006	HIA+
F 20 %Bioavaibility	0.983	Poor Bioavaibility	0.005	Excelent Bioavaibility
F 30 %Bioavaibility	0.007	Excelent Bioavaibility	0.003	Excelent Bioavaibility
Caco-2 Permeability	-4.482	Permeable	-4.543	Permeable
MDCK Permeability	4.1e-05	Permeable	1.7e-05	Permeable
P-glycoprotein substrate	0.983	Substrate	0.0	Non-Substrate
P-glycoprotein inhibitor	0.002	Non- inhibitor	0.001	Non- inhibitor
Distribution				
Blood-brain barrier Penetration	0.991	BBB-	0.842	BBB-
Metabolisom				
CYP1A2 inhibitor	0.911	Inhibitor	0.885	Inhibitor
CYP1A2 substrate	0.7	Substrate	0.482	Non-substrate
CYP2C19 inhibitor	0.403	Non-inhibitor	0.948	Inhibitor
CYP2C19 substrate	0.461	Non-substrate	0.355	Non-substrate
CYP2C9 inhibitor	0.061	Non-inhibitor	0.724	Inhibitor
CYP2C9 substrate	0.058	Non-substrate	0.173	Non-substrate
CYP2D6 inhibitor	0.506	Inhibitor	0.208	Non-inhibitor
CYP2D6 substrate	0.226	Non-substrate	0.476	Non-substrate
CYP3A4 inhibitor	0.016	Non-inhibitor	0.126	Non-inhibitor
CYP3A4 substrate	0.431	Non-substrate	0.334	Non-substrate
Toxicity				
AMES toxicity	0.163	Non-Ames Toxicity	0.042	Non-Ames Toxicity
Skin sensitization	0.884	Skin sensitizer	0.824	Skin sensitizer
Drug induced liver injury (DILI)	0.765	DILI	0.697	DILI

The transport of drugs across cellular membranes is not solely dependent on their chemical properties, but also on their lipophilicity—a property that significantly influences the transfer of substances within various settings, including the delivery of bioactive compounds (Chmiel *et al.*, 2019). Lipophilicity, also known as LogP, measure the balance between the concentrations of a compound in both oil and liquid phases at equilibrium (Chandrasekaran *et al.*, 2018). According to Waring (2010), compounds with lower logP values (<3) were more likely to be soluble in 50% of cases, while compounds with high logP values ($>$ than 3) showed only about 1% of significant solubility. In this study, each constituent of Ph₂Sn(*N*-ethyl-*N*-benzylidithiocarbamate) exhibit the capacity to

traverse lipid membranes ($\log P \leq 5$). However, the ligands present in these complexes may play a pivotal role in determining their overall lipophilicity, as they tend to be more soluble ($\log P < 3$). This observation supporting previous studies that ligand significantly influence the lipophilicity and stability of metal complexes (Galanski *et al.*, 2005).

Although lipophilicity has been identified as a key determinant of drug uptake and metabolism, but it may also contribute to off-target binding or promiscuity, thereby increasing the likelihood of adverse effects (Stephens *et al.*, 2014). Previous studies have underscored the significance of drug lipid solubility (lipophilicity) as a possible predictor of drug-induced liver injury (DILI). Research by Chen

et al., (2013) have revealed that combining high daily doses (≥ 100 mg) with high lipophilicity ($\text{LogP} \geq 3$) is linked to an elevated danger of DILI.

The intestinal epithelial barrier is requisite in governing the entry of substances into the systemic circulation by controlling their passage through this membrane. To elucidate the absorptive properties of compound, two established models such as Human Intestinal Absorption (HIA) and Caco-2 permeability measurements were employed (Guan *et al.*, 2019). Notably, $\text{Ph}_2\text{Sn}(N\text{-ethyl-}N\text{-benzylidithiocarbamate})$ exhibited a favorable outcome in both the Caco-2 and HIA+, indicating that this compound is highly permeable across the GI epithelium. According to established criteria, a compound is deemed to possess adequate Caco-2 permeability if its predicted value exceeds 8×10^8 cm/s, while a molecule with an Intestinal Absorption rate below 30% is classified as poorly absorbed (Flores-Holguín *et al.*, 2021).

Meanwhile, the cytochrome P450 (CYP) enzyme system was predominantly involved in Phase I oxidative biotransformational processes within the body, with specific isoforms such as 1A2, 2C9, 2C19, 2D6, and 3A4 playing crucial roles in these processes (Sychev *et al.*, 2018). Notably, our newly developed compound exhibited no inhibition of cytochrome P450 (CYP450) enzymes across multiple classes, thereby preventing any disruptions in the metabolic processing of other drugs (Syed Annuar *et al.*, 2022).

P-glycoprotein functions as a cellular barrier by expelling harmful substances from cells through an active transport mechanism (Flores-Holguín *et al.*, 2021). According to computational predictions, the Ph_2Sn may serve as both a substrate and non-inhibitor for P-glycoprotein, with dithiocarbamate acting as a non-substrate and non-inhibitor of this protein. This compound has been found to exhibit BBB+, indicating its potential ability to crossing the blood-brain barrier (BBB). Most xenobiotics that enter the central nervous system (CNS) do so via passive diffusion, with greater lipid solubility leading to improved CNS penetration. However, excessively high lipophilicity can lead to increased nonspecific binding to plasma proteins. Studies have identified xenobiotics with moderate lipophilic properties

(logP/logD range of 1.7 to 2.8) as having the greatest uptake into the CNS (Chmiel *et al.*, 2019).

CONCLUSION

In summary, we report the successful synthesis of $\text{Ph}_2\text{Sn}(N\text{-ethyl-}N\text{-benzylidithiocarbamate})$ employing an insitu approach and characterisation of this compound through various spectroscopy analyses. Specifically, our findings indicate that the ligand coordinates bidentately to the tin metal center of the organotin(IV) moiety through the $\nu(\text{C}=\text{S})$ bond, as substantiated by the singular peak in the IR spectrum. Furthermore, ^{119}Sn NMR analysis confirmed a hexacoordinate arrangement around the Sn atom. Besides, cytotoxic screening of this compound revealed its exceptionally high efficacy relative to existing drugs. This work underscores the potential of diphenyltin(IV) dithiocarbamate compound as leads in anticancer drug discovery, while also offering valuable insights into the pharmacokinetics of this compound, which can inform future developments and refinements thereof.

ACKNOWLEDGMENT

We extend our heartfelt thanks to the Malaysian Ministry of Higher Education (MOHE) for granting us financial aid through the Fundamental Research Grant Scheme (FRGS) with grant number FRGS/1/2021/STG04/UKM/02/5, as well as the Faculty of Health Sciences at Universiti Kebangsaan Malaysia for their generous support of this research endeavor. Besides, we extend our sincere appreciation to the Faculty of Health Sciences at Universiti Kebangsaan Malaysia and the School of Medical and Life Sciences (SMLS) at Sunway University for providing access to their state-of-the-art facilities and infrastructure. Additionally, we are grateful for the expert technical support offered by the Centre for Research and Instrumentation Management (CRIM) and the Organic Synthesis Research Laboratory at the Institute of Science (UiTM), which greatly facilitated the analysis and interpretation of data generated during the course of this investigation.

Conflicts of Interest

In this study, all participating researchers have disclosed that they do not possess any conflicting interests that could potentially influence the results or interpretation of our findings.

REFERENCES

1. Abd Aziz, N. A.; Awang, N.; Chan, K. M.; Kamaludin, N. F.; Mohamad Anuar, N. N., *Molecules.*, **2023**, *28*, 5841.
2. Adeyemi, J. O.; Olasunkanmi, L. O.; Fadaka, A. O.; Sibuyi, N. R. S.; Oyedeji, A. O.; Onwudiwe, D. C., *Molecules.*, **2022**, *27*, 2947.
3. Adeyemi, J. O.; Onwudiwe, D. C., *Pol. J. Environ. Stud.*, **2020**, *29*, 2525–2532.
4. Adeyemi, J. O.; Onwudiwe, D. C.; Nundkumar, N.; Singh, M., *Open Chem.*, **2020**, *18*, 453–462.
5. Ajibade, P. A.; Onwudiwe, D. C.; Moloto, M., *J. Polyhedron.*, **2011**, *30*, 246–252.
6. Banti, C. N.; Hadjidakou, S. K.; Sismanoglu, T.; Hadjiliadis, N., *J. Inorg. Biochem.*, **2019**, *194*, 114–152.
7. Bunn, P. A. The expanding role of cisplatin in the treatment of non-small-cell lung cancer., *Semin. Oncol.*, **1989**, *16*, 10–21.
8. Chandrasekaran, B.; Abed, S. N.; Al-Attraqchi, O.; Kuche, K.; Tekade, R. K., *Dosage Form Design Parameters.*, **2018**, 731–755.
9. Chen, M.; Borlak, J.; Tong, W., *Hepatology.*, **2013**, *58*, 388-96.
10. Chmiel, T.; Mieszkowska, A.; Kempka, Kupczyk, D.; Kot-Wasik, A.; Namieńnik, J.; Mazerska, Z., *Microchemical Journal.*, **2019**, *146*, 393-406.
11. Flores-Holguín, N.; Frau, J.; Glossman-Mitnik, D., *Front. Chem.*, **2021**, *9*, 708364.
12. Galanski, M. S.; Jakupec, M. A.; Keppler, B. K., *Curr. Med. Chem.*, **2005**, *12*, 2075–2094.
13. Guan, L.; Yang, H.; Cai, Y.; Sun, L.; Di, P.; Li, W.; Liu, G.; Tang, Y., *Medchemcomm.*, **2019**, *10*, 148-157.
14. Hadjidakou, S. K.; Hadjiliadis, N., *Coord. Chem. Rev.*, **2009**, *253*, 235-249.
15. Haezam, F. N.; Awang, N.; Kamaludin, N. F.; Mohamad, R., *Saudi J. Biol. Sci.*, **2021**, *28*, 3160–3168.
16. Iqbal, M.; Ali, S.; Haider, A.; Khalid, N., *Rev. Inorg. Chem.*, **2017**, *37*, 51–70.
17. Islam, M. K.; Baek, A. R.; Sung, B.; Yang, B. W.; Choi, G.; Park, H. J.; Kim, Y. H.; Kim, M.; Ha, S.; Lee, G. H.; Kim, H. K.; Chang, Y., *Pharmaceuticals.*, **2021**, *14*, 832.
18. Kadu, R.; Roy, H.; Singh, V. K., *Appl. Organomet. Chem.*, **2015**, *29*, 746–755.
19. Kamaludin, N. F.; Awang, N.; Baba, I.; Hamid, A.; Meng, C. K., *Pak. J. Biol. Sci.*, **2013**, *16*, 12–21.
20. Khan, S.; Nami, S. A. A.; Siddiqi, K. S., *J. Organomet. Chem.*, **2008**, *693*, 1049–1057.
21. Kumar Singh, A.; Kumar, A.; Singh, H.; Sonawane, P.; Pathak, P.; Grishina, M.; Pal Yadav, J.; Verma, A.; Kumar, P., *Chem. Biodivers.*, **2023**, *20*, e202300061.
22. Liu, K.; Yan, H.; Chang, G.; Li, Z.; Niu, M.; Hong, M., *Inorganica Chim. Acta.*, **2017**, *464*, 137–146.
23. Martini, P.; Boschi, A.; Marvelli, L.; Uccelli, L.; Carli, S.; Cruciani, G.; Marzola, E.; Fantinati, A.; Esposito, J.; Duatti, A., *Molecules.*, **2021**, *26*, 5954.
24. Mohamad, R.; Awang, N.; Kamaludin, N. F., *Res. J. Pharm. Biol. Chem. Sci.*, **2016**, *7*(2), 1920–1925.
25. Mosmann, T., *J. Immunol. Methods.*, **1983**, *65*, 55–63.
26. Muhammad, N.; Ahmad, M.; Sirajuddin, M.; Ali, Z.; Tumanov, N.; Wouters, J.; Chafik, A.; Solak, K.; Mavi, A.; Muhammad, S.; Shujah, S.; Ali, S.; Al-Sehemi, A. G., *Front. Pharmacol.*, **2022**, *13*, 864336.
27. Muthalib, A. F. A.; Baba, I., *AIP Conference Proceedings.*, **2014**, *1614*, 237–243.
28. Odularu, A. T.; Ajibade, P. A., *Bioinorg. Chem. Appl.*, **2019**, *2019*, 1–15.
29. Onwudiwe, D. C.; Hrubaru, M.; Ebenso, E. E., *J. Nanomater.*, **2015**, *2015*, 1–9.
30. Onwudiwe, D. C.; Nthwane, Y. B.; Ekenia, A. C.; Hosten, E., *Inorganica Chim. Acta.*, **2016**, *447*, 134-141.
31. Oun, R.; Moussa, Y. E.; Wheate, N., *J. Dalton Trans.*, **2018**, *47*, 6645–6653.
32. Prakasam, B. A.; Ramalingam, K.; Baskaran, R.; Bocelli, G.; Cantoni, A., *Polyhedron.*, **2007**, *26*, 1133–1138.
33. Rasli, N. R.; Hamid, A.; Awang, N.; Kamaludin, N. F., *Molecules.*, **2023**, *28*, 3376.
34. Stephens, C.; Andrade, R. J.; Lucena, M. I., *Curr. Opin. Allergy Clin. Immunol.*, **2014**, *14*, 286-292.
35. Sychev, D. A.; Ashraf, G. M.; Svistunov, A. A.; Maksimov, M. L.; Tarasov, V. V.; Chubarev, V. N.; Otdelenov, V. A.; Denisenko, N. P.; Barreto, G. E.; Aliev, G., *Drug Des. Devel. Ther.*, **2018**, *12*, 1147–1156.
36. Syed Annuar, S. N.; Kamaludin, N. F.; Awang, N.; Chan, K. M., *Food Chem. Toxicol.*, **2022**, *168*, 113336.
37. Waring, M., *J. Expert Opin. Drug Discov.*, **2010**, *5*, 235–248.
38. Zhuang, W. R.; Wang, Y.; Cui, P. F.; Xing, L.; Lee, J.; Kim, D.; Jiang, H. L.; Oh, Y. K., *Journal of Controlled Release.*, **2019**, *294*, 311-326.